Diagn Interv Radiol 2015; 21:105–110

ABDOMINAL IMAGING
PICTORIAL ESSAY

Imaging of aberrant left gastric vein and associated pseudolesions of segments II and III of the liver and mimickers

Emre Unal, Mustafa Nasuh Ozmen, Deniz Akata, Musturay Karcaaltincaba

ABSTRACT
We present imaging findings of aberrant left gastric vein (ALGV) and associated pseudolesions and mimickers including metastases and focal nodular hyperplasia. ALGV is formed due to interrupted involution of anastomotic omental veins, and it can drain into left portal vein or segments II and III of the liver as third inflow. Focal fat, focal fat sparing, and perfusion changes can be seen due to the presence of ALGV, which can mimic metastasis in cancer patients. ALGV may also serve as a pathway for direct tumor spread into the liver in patients with gastric cancer. Magnetic resonance imaging can be used as a problem solving tool in the presence of equivocal findings on ultrasonography and computed tomography.

From the Department of Radiology (M.K. ✉ *musturayk@yahoo.com*), Hacettepe University, School of Medicine, Ankara, Turkey.

Received 17 August 2014, revision requested 25 August 2014, final revision received 16 September 2014, accepted 17 September 2014.

Published online 13 February 2015.
DOI 10.5152/dir.2014.14360

Pseudolesions of the liver are a well-known issue and have been reported in the literature. These pseudolesions are caused by aberrant hepatopedal venous flow other than portal venous system, also known as third inflow. Third inflow is most commonly due to aberrant right gastric, paraumbilical, and cholecystic veins (1–3). Pseudolesions caused by aberrant left gastric vein (ALGV) are considered to be a more rare entity (4).

The purpose of this study is to illustrate ALGV drainage into the liver and associated pseudolesions of segments II and III of the liver. In addition, we illustrate imaging findings of the mimickers of these pseudolesions.

Embryology and anatomy

The left gastric vein receives branches of the inferior paraesophageal region and minor curvature of the stomach. Thereafter, it runs along the hepatogastric ligament and merges with the left aspect of the portal vein or confluence of the portal and splenic veins. The right gastric vein also receives blood from minor curvature of the stomach and merges with the right aspect of the portal vein.

Aberrant left and right gastric veins develop due to morphogenetic changes during the developmental process in the early embryonic life (5). The main cause is interrupted involution of the anastomotic omental veins, so that typical left gastric vein does not form. Anastomotic omental veins are the anastomoses between primitive foregut venous plexus and ductus venosus, which normally exist during early embryonic life (5, 6).

Types

Depending on the course and entrance to the liver, ALGVs have been classified into three types (Fig. 1). Type 1 vein acts as a pure accessory portal vein, which branches out and flows through the sinusoids (Fig. 2a). Type 2 vein has a parenchymatous distribution with anastomosis to portal vein (Fig. 2b). Type 3 vein has a more cranial course with anastomosis to intrahepatic portal vein branches (Fig. 2c) (5, 7). However, there is no classification of ALGV in the literature based on radiologic findings. ALGV can be important in patients with main portal vein thrombosis and can restore portal flow in the left lobe of the liver (Fig. 2d, 2e).

In patients with occluded superior vena cava, ALGV can be visible due to retrograde flow of iodinated contrast into the liver, and related perfusion changes can mimic a hypervascular liver lesion (Fig. 3).

Fat sparing

Focal fat sparing in diffuse fatty liver is reported and well described in the literature (8–12). It is speculated that fat sparing may occur due to altered fatty acid and triglyceride levels associated with different compositions of hormones in the portal flow and third inflow (2).

Liver parenchyma adjacent to the gallbladder fossa and falciform ligament, dorsal aspect of segment IV, and subcapsular areas are the most common locations for fat sparing that is attributed to the cholecystic venous, paraumbilical venous, aberrant right gastric venous, and capsular venous drainage, respectively (1, 2, 13). However, ALGV drainage may also cause fat

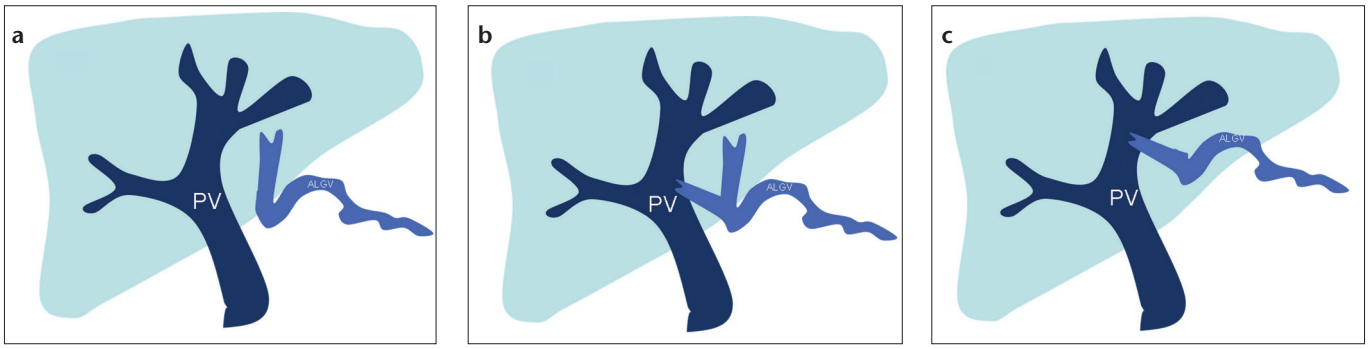

Figure 1. a–c. Schematic drawing shows the types of aberrant left gastric vein (ALGV). Type 1 vein **(a)** acts as a pure accessory portal vein (PV) which branches out and flows through the sinusoids. Type 2 vein **(b)** has a parenchymatous distribution with anastomosis to PV. Type 3 vein **(c)** has a more cranial course with anastomosis to intrahepatic PV branches.

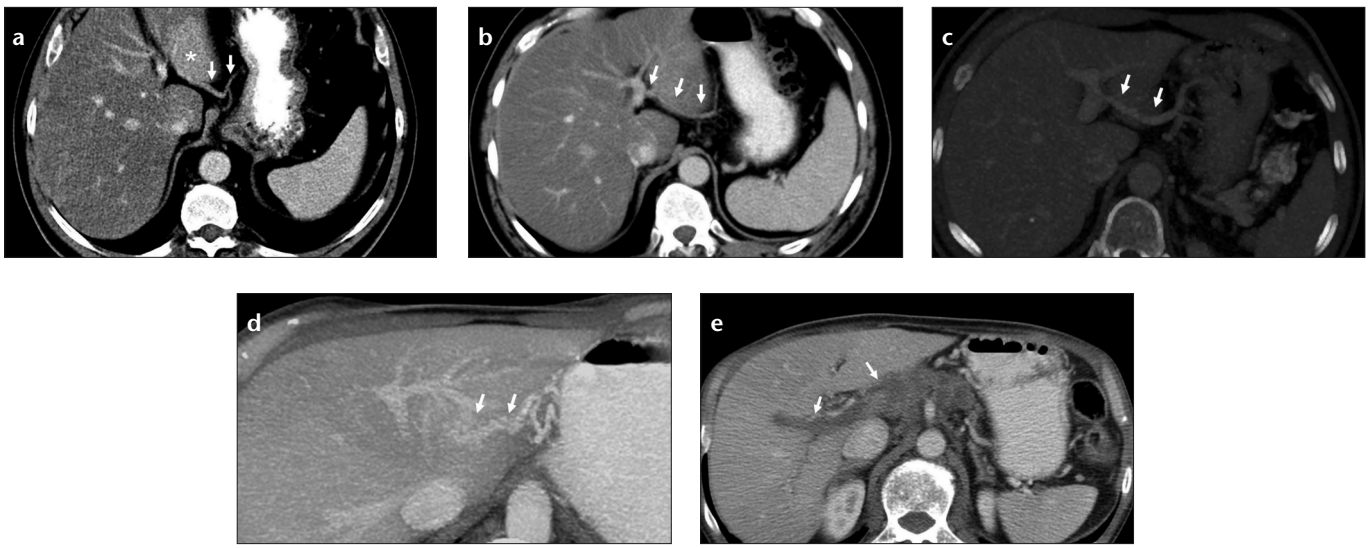

Figure 2. a–e. Images of ALGV types from different patients. Axial CT image **(a)** shows type 1 ALGV (*arrows*) which enters the liver parenchyma and leads to fat sparing (*asterisk*) at the posterior aspect of segments II and III. Axial CT image **(b)** shows type 2 ALGV (*arrows*), which courses through the parenchyma with anastomosis to the left portal vein. Axial maximum intensity projection (MIP) image **(c)** shows type 3 ALGV (*arrows*) with anastomosis to the left portal vein. Left portal vein opacification by ALGV in a patient with main portal vein thrombosis **(d, e)**. Axial MIP CT image **(d)** shows anastomosis between ALGV (*arrows*) and left portal vein branch. Axial CT image **(e)** shows thrombosis of the main and right portal veins (*arrows*).

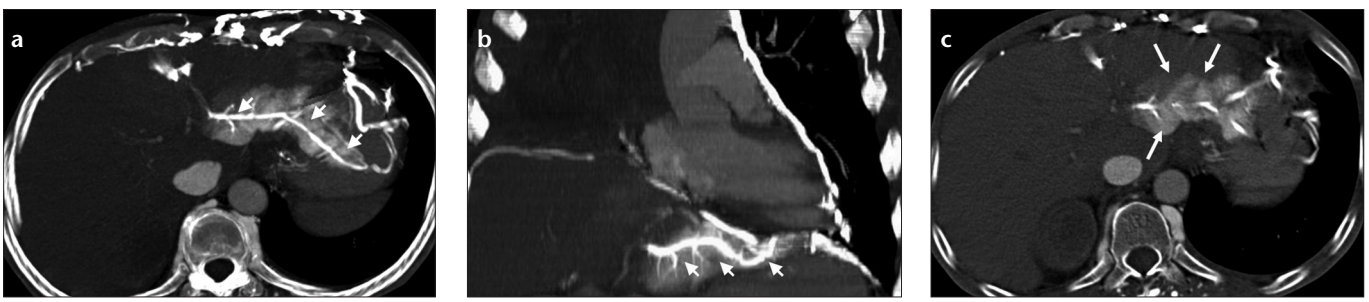

Figure 3. a–c. A lung cancer patient with superior vena cava occlusion and perfusion change at the posterior aspect of left lobe of the liver noted on chest CT. Axial **(a)** and coronal **(b)** MIP CT images show hyperdense appearance and contrast reflux to ALGV (*arrows*) from collateral flow through anastomosis between pericardiophrenic and gastric veins. Axial CT image **(c)** of the same patient shows parenchymal hyperdensity which may mimic hypervascular lesion and focal fat spared area. Filling of ALGV leads to the diagnosis.

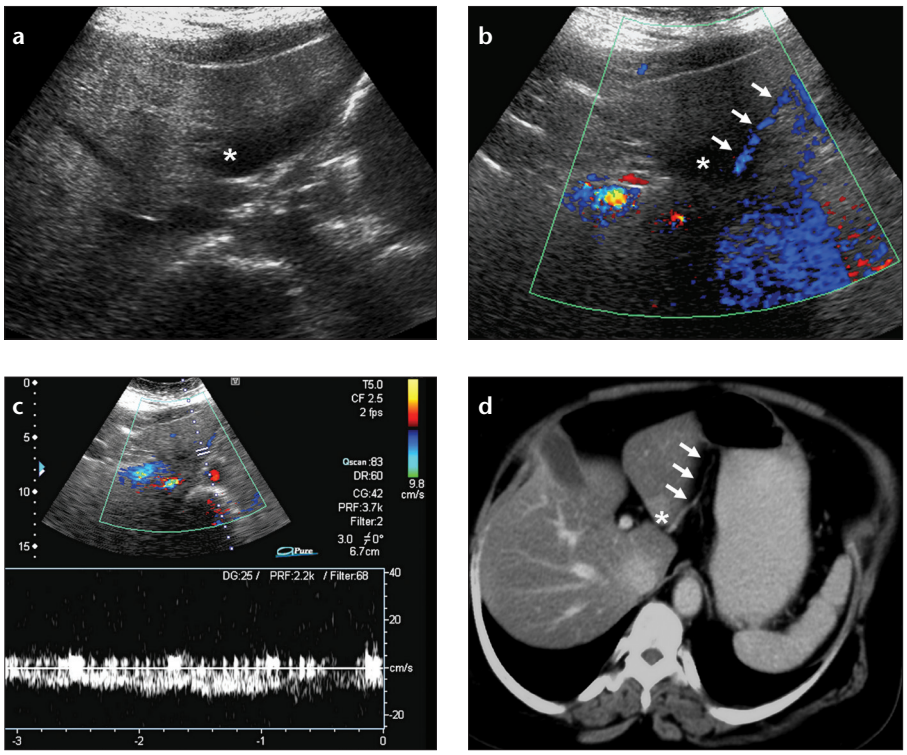

Figure 4. a–d. Focal fat spared area with accompanying ALGV in a breast cancer patient. Axial US **(a)** and color Doppler US **(b)** images show focal fat spared area (*asterisk*) and the course of ALGV (*arrows*). Venous flow pattern is demonstrated by pulsed-wave Doppler US image **(c)**. Axial CT image **(d)** reveals focal fat spared area, seen as relatively increased density (*asterisk*), and the course of ALGV (*arrows*).

sparing at the posterior aspect of segments II and III of the liver, which is an uncommon location for fat sparing. Differentiation of focal fat spared area from tumor or any other true lesion is a diagnostic challenge in a cancer patient, particularly when the fat sparing occurs in an uncommon location.

On ultrasonography (US) focal fat sparing can be seen as a geographic or nodular hypoechoic area in a background of hyperechogenic fatty liver (Fig. 4a). Doppler US can demonstrate ALGV in patients with fat sparing and this information can increase the diagnostic confidence (Fig. 4b, 4c). In pre- and postcontrast computed tomography (CT) scans, fat spared area is seen as a relatively focal hyperdense area in the fatty liver (Fig. 4d). Magnetic resonance imaging (MRI) can be used as a problem solving tool in cancer patients with equivocal findings (Fig. 5). In- and out-of-phase T1-weighted images can demonstrate focal lack of signal drop on opposed-phase images in the presence of focal fat sparing (Fig. 5c, 5d). In patients with very high liver fat content, fat spared area can be seen as a relatively hypointense area on

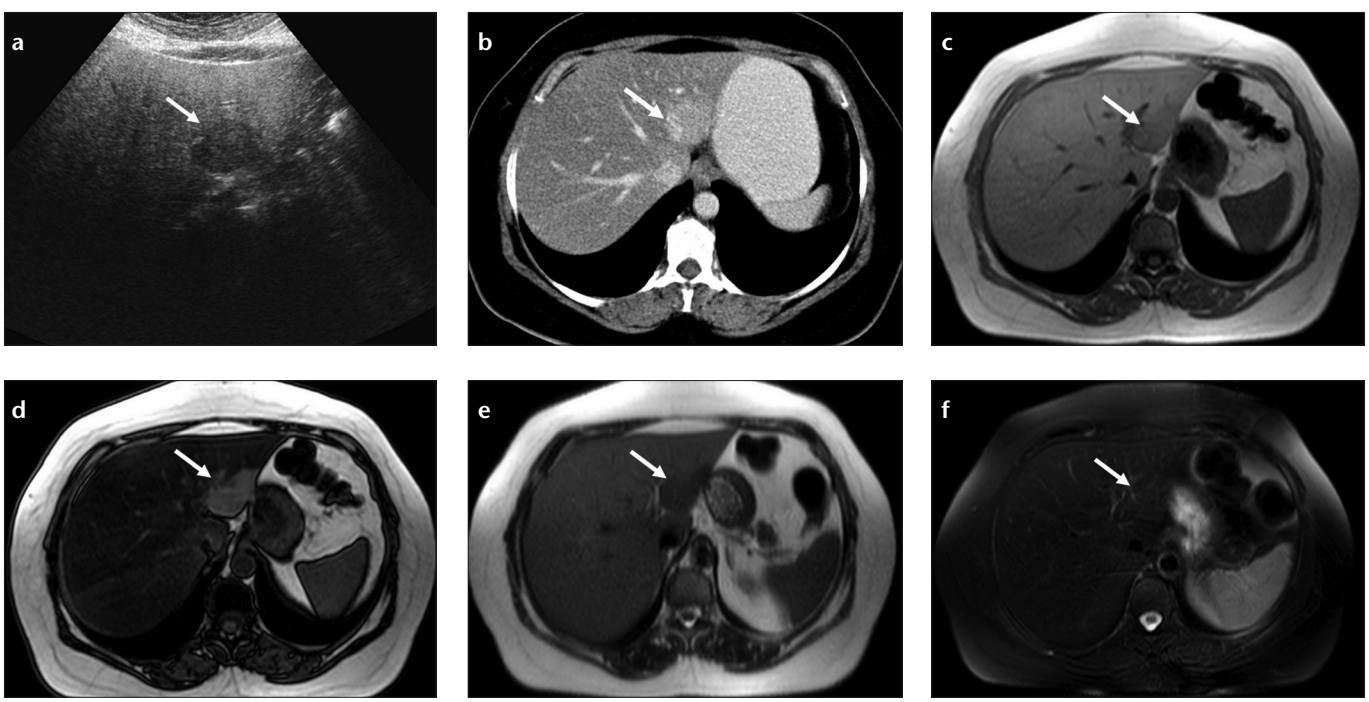

Figure 5. a–f. Nodular focal fat spared area in a patient with melanoma. Axial US image **(a)** shows hypoechoic lesion *(arrow)* in a fatty liver and CT image **(b)** shows hyperdense area at the posterior aspect of segments II and III *(arrow)*. In-phase **(c)** and out-of-phase **(d)** T1-weighted images show focal fat spared area by signal reduction in the whole liver parenchyma except for the fat spared area on the out-of-phase image *(arrows)*. Severe steatosis causes increased signal of the liver on T2-weighted image **(e)** and the spared area (normal liver) appears hypointense; this contrast difference disappears on fat-saturated T2-weighted image **(f)**.

T2-weighted images, which disappears on fat-saturated T2-weighted images (Fig. 5e, 5f).

Focal fat

Focal fatty area is another entity seen at similar locations where fat sparing occurs. Presence of focal fatty infiltration in these areas disproves the aforementioned hormonal hypothesis (14). In our experience, areas of third inflow behave opposite to the rest of the liver supplied by portal inflow. Fatty areas show low attenuation values on CT scan because of increased fat content compared to the rest of the liver (Fig. 6).

Tumor spread

Gastric carcinomas may spread locally via lymphovascular system. Left and right gastric veins are commonly affected, when local vascular spread occurs. Along the course of left gastric vein, hepatogastric ligament and periportal space may be affected by tumor invasion and can result in biliary obstruction and portal vein occlusion. Segments II and III of the liver may be affected by direct tumor spread via ALGV (Fig. 7).

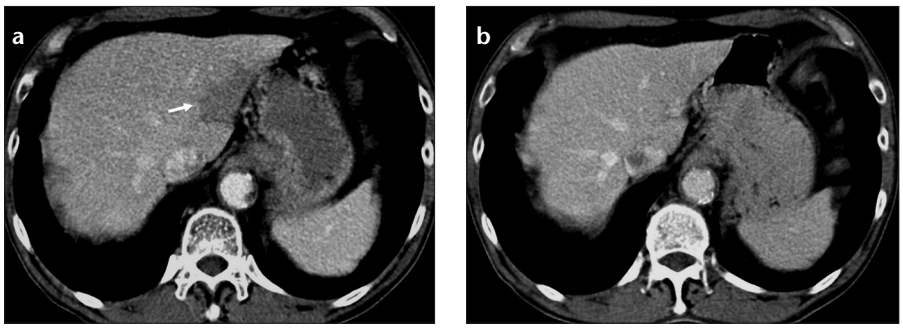

Figure 6. a, b. Focal fat at the posterior aspect of segments II and III of the liver. Axial CT image **(a)** of a lymphoma patient shows focal hypodensity that does not displace small vascular structures. Axial CT image **(b)** of the same patient two years later shows disappearance of focal fat.

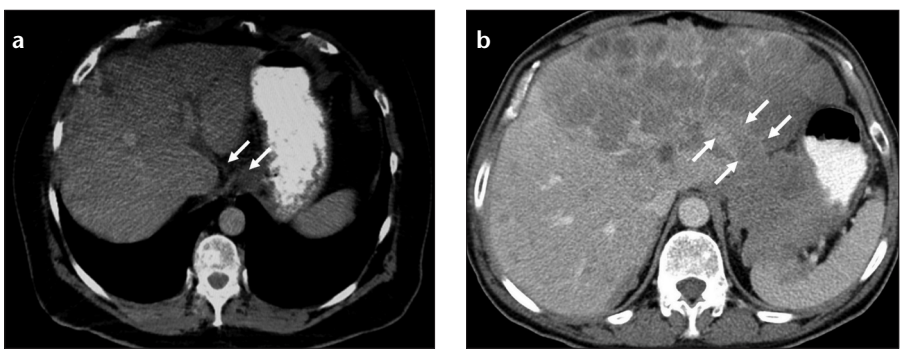

Figure 7. a, b. Direct spread of gastric carcinoma into the liver via ALGV. Axial CT image **(a)** shows a mass at esophagogastric junction and tumor invasion of ALGV (*arrows*). Axial CT image **(b)** in another patient with gastric carcinoma shows tumor extension and metastasis to the left lobe of the liver via ALGV (*arrows*).

Mimickers

Focal fat sparing and fatty infiltration areas are considered to be pseudolesions. However, it should be kept in mind that, focal true liver lesions may manifest with similar findings. Focal nodular hyperplasia may mimic focal fat sparing or perfusion changes due to ALGV, because of its homogeneous hypervascularity (Fig. 8a) (15). MRI should be preferred in such cases and presence of scar on T2-weighted images and hyperintensity on hepatobiliary phase T1-weighted images after injection of hepatocyte specific agents can be helpful in making the diagnosis (Fig. 8b, 8c) (16, 17). Metastasis can mimic focal fat and fat sparing. Hypovascular solitary metastasis to the posterior aspect of segments II and III of the liver can mimic focal fat, and presence of mass effect and associated biliary dilatation can be used for diagnosis of metastases (Fig. 9). Steatotic hepatic adenoma, hepatocellular carcinoma with fatty degeneration, and perilesional fat in neuroendocrine metastases may also mimic focal fat (12). Rarely, fat containing metastases due to liposarcoma can be seen at this location and may mimic focal fatty infiltration due to similar appearance on US and CT (Fig. 10) (8, 18).

Conclusion

ALGV-associated hepatic pseudolesions involving posterior aspect of segments II and III of the liver can mimic

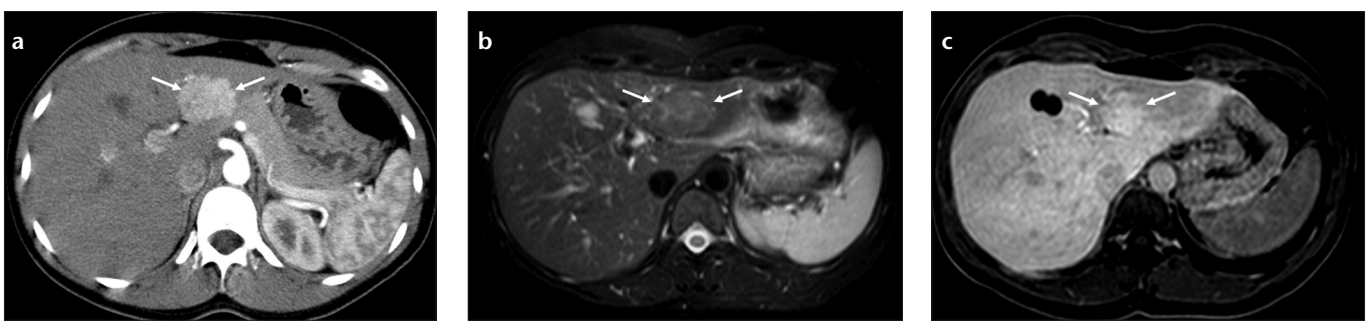

Figure 8. a–c. Focal nodular hyperplasia mimicking perfusion change and fat spared area at the posterior aspect of segments II and III. Axial CT image **(a)** shows an arterial enhancing mass *(arrows)* in a patient with history of papillary thyroid carcinoma. Axial T2-weighted fat saturated image **(b)** shows a slightly hyperintense lesion with a central scar *(arrows)*. Hepatobiliary phase T1-weighted image **(c)** shows focal gadobenate dimeglumine uptake consistent with focal nodular hyperplasia *(arrows)*.

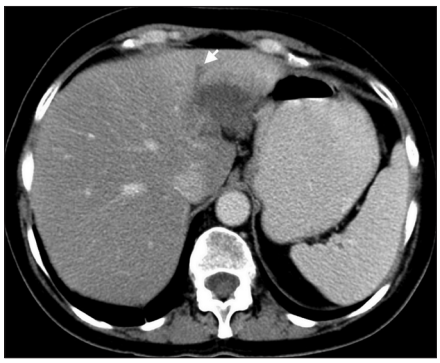

Figure 9. A patient with breast carcinoma and solitary metastasis to segments II and III of the liver mimicking focal fat. Axial CT image shows a hypodense lesion and accompanying bile duct dilatation (*arrow*), which is not seen in the presence of focal fat.

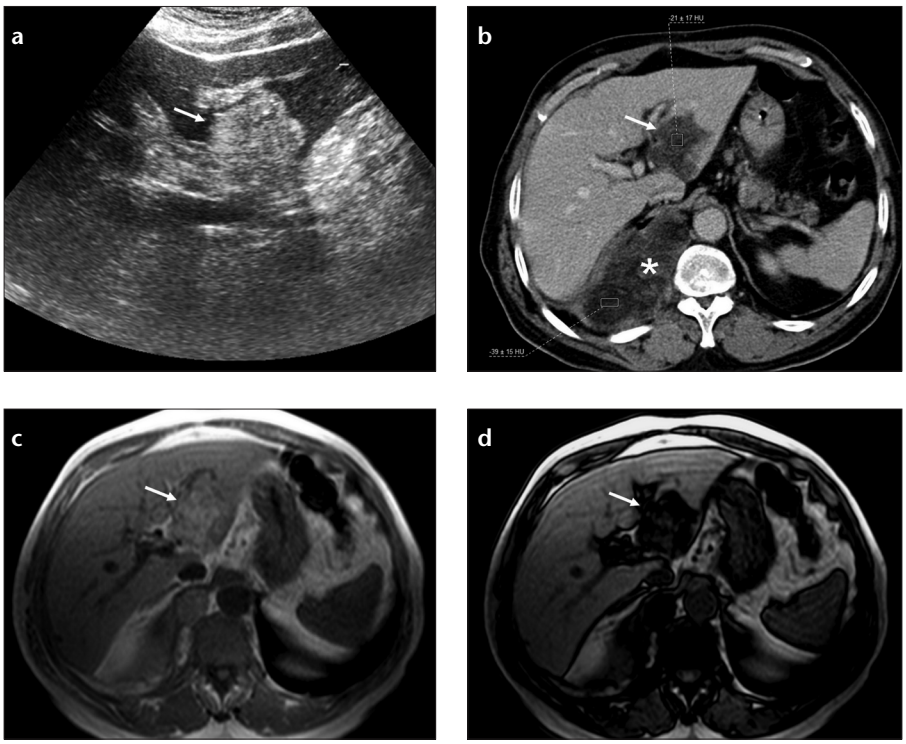

Figure 10. a–d. Liposarcoma metastasis mimicking focal fat. Axial US image **(a)** of the liver shows a hyperechogenic mass at segments II and III of the liver *(arrow)*. Axial CT image **(b)** shows fat density of the mass *(arrow)* and right thoracic primary mass (*asterisk*). In-phase **(c)** and out-of-phase **(d)** T1-weighted images show signal reduction in the fat containing mass due to coexistence of fat and solid parts *(arrows)*.

metastasis, and MRI can be used to distinguish between pseudolesions and true lesions. Presence of ALGV in gastric cancer patients can lead to direct tumor spread into the liver.

Conflict of interest disclosure

The authors declared no conflicts of interest.

References

1. Hiwatashi A, Yoshimitsu K, Honda H, et al. Pseudolesion in segment II of the liver observed on CT during arterial portography caused by the aberrant left gastric venous drainage. Abdom Imaging 1999; 24:357–359. [CrossRef]
2. Matsui O, Takahashi S, Kadoya M, et al. Pseudolesion in segment IV of the liver at CT during arterial portography - correlation with aberrant gastric venous drainage. Radiology 1994; 193:31–35. [CrossRef]
3. Yoshimitsu K, Honda H, Kaneko K, et al. Anatomy and clinical importance of cholecystic venous drainage: Helical CT observations during injection of contrast medium into the cholecystic artery. AJR Am J Roentgenol 1997; 169:505–510. [CrossRef]
4. Terayama N, Matsui O, Tatsu H, Gabata T, Kinoshita A, Hasatani K. Focal sparing of fatty liver in segment II associated with aberrant left gastric vein. Br J Radiol 2004; 77:150–152. [CrossRef]
5. Nebotcegarra J, Domenechmateu JM. Intrahepatic termination of the left gastric vein (vena gastrica sinistra) - a new case of this unusual anatomic variation. Anat Anz 1986; 161:309–315.
6. Deneve E, Caty L, Fontaine C, Guillem P. Simultaneous aberrant left and right gastric veins draining directly into the liver. Ann Anat 2003; 185:263–266. [CrossRef]
7. Reichardt W, Butzow GH, Erbe W. Anomalous venous connections involving the portal system. Cardiovasc Radiol 1979; 2:41–46. [CrossRef]
8. Pokharel SS, Macura KJ, Kamel IR, Zaheer A. Current MR imaging lipid detection techniques for diagnosis of lesions in the abdomen and pelvis. Radiographics 2013; 33:681–702. [CrossRef]
9. Valls C, Iannacconne R, Alba E, et al. Fat in the liver: Diagnosis and characterization. Eur Radiol 2006; 16:2292–2308. [CrossRef]
10. Cassidy FH, Yokoo T, Aganovic L, et al. Fatty liver disease: MR imaging techniques for the detection and quantification of liver steatosis. Radiographics 2009; 29:231–260. [CrossRef]
11. Arai K, Matsui O, Takashima T, Ida M, Nishida Y. Focal spared areas in fatty liver caused by regional decreased portal flow. AJR Am J Roentgenol 1988; 151:300–302. [CrossRef]
12. Karcaaltincaba M, Akhan O. Imaging of hepatic steatosis and fatty sparing. Eur J Radiol 2007; 61:33–43. [CrossRef]
13. Ohashi I, Ina H, Gomi N, et al. Hepatic pseudolesion in the left lobe around the falciform ligament at helical CT. Radiology 1995; 196:245–249. [CrossRef]
14. Paulson EK, Baker ME, Spritzer CE, Leder RA, Gulliver DJ, Meyers WC. Focal fatty infiltration: A cause of nontumorous defects in the left hepatic lobe during CT arterial portography. J Comput Assist Tomogr 1993; 17:590–595. [CrossRef]
15. Brancatelli G, Federle MP, Grazioli L, Blachar A, Peterson MS, Thaete L. Focal nodular hyperplasia: CT findings with emphasis on multiphasic helical CT in 78 patients. Radiology 2001; 219:61–68. [CrossRef]

16. Grazioli L, Morana G, Kirchin MA, Schneider G. Accurate differentiation of focal nodular hyperplasia from hepatic adenoma at gadobenate dimeglumine-enhanced MR imaging: Prospective study. Radiology 2005; 236:166–177. [CrossRef]

17. Thomeer MG, E Bröker ME, de Lussanet Q, et al. Genotype-phenotype correlations in hepatocellular adenoma: an update of MRI findings. Diagn Interv Radiol 2014; 20:193–199. [CrossRef]

18. Basaran C, Karcaaltincaba M, Akata D, et al. Fat-containing lesions of the liver: Cross-sectional imaging findings with emphasis on MRI. AJR Am J Roentgenol 2005; 184:1103–1110. [CrossRef]